

Published in final edited form as:

J Mol Cell Cardiol. 2013 December ; 65: . doi:10.1016/j.yjmcc.2013.09.013.

Loss of NHE1 activity leads to reduced oxidative stress in heart and mitigates high-fat diet-induced myocardial stress

Vikram Prasad^a, John N. Lorenz^b, Marian L. Miller^c, Kanimozhi Vairamani^a, Michelle L. Nieman^b, Yigang Wang^d, and Gary E. Shull^a

^aDepartment of Molecular Genetics, Biochemistry, and Microbiology, University of Cincinnati College of Medicine, Cincinnati, OH, 45267-0524

^bDepartment of Molecular and Cellular Physiology, University of Cincinnati College of Medicine, Cincinnati, OH, 45267-0524

^cDepartment of Environmental Health, University of Cincinnati College of Medicine, Cincinnati, OH, 45267-0524

^dDepartment of Pathology and Laboratory Medicine, University of Cincinnati College of Medicine, Cincinnati, OH, 45267-0524

Abstract

Acute inhibition of the NHE1 Na⁺/H⁺ exchanger protects against ischemia-reperfusion injury and chronic inhibition attenuates development of cardiac hypertrophy and failure. To determine the cardiac effects of chronic inhibition of NHE1 under non-pathological conditions we used NHE1-null mice as a model of long-term NHE1 inhibition. Cardiovascular performance was relatively normal in *Nhe1*^{-/-} mice although cardiac contractility and relaxation were slightly improved in mutant mice of the FVB/N background. GSH levels and GSH:GSSG ratios were elevated in *Nhe1*^{-/-} hearts indicating an enhanced redox potential. Consistent with a reduced need for antioxidant protection, expression of heat shock proteins Hsp60 and Hsp25 was lower in *Nhe1*^{-/-} hearts. Similarly, expression of mitochondrial superoxide dismutase 2 was reduced, with no increase in expression of other ROS scavenging enzymes. GLUT1 levels were increased in *Nhe1*^{-/-} hearts, the number of lipid droplets in myocytes was reduced, and PDK4 expression was refractory to high-fat diet-induced upregulation observed in wild-type hearts. High-fat diet-induced stress was attenuated in *Nhe1*^{-/-} hearts, as indicated by smaller increases in phosphorylation of Hsp25 and α -B crystallin, and there was better preservation of insulin sensitivity, as evidenced by PKB/Akt phosphorylation. Plasma glucose and insulin levels were lower and high-fat diet-induced hepatic lipid accumulation was reduced in *Nhe1*^{-/-} mice, demonstrating extracardiac effects of NHE1 ablation. These data indicate that long-term ablation of NHE1 activity increases the redox potential, mitigates high-fat diet-induced myocardial stress and fatty liver disease, leads to better preservation of insulin sensitivity, and may alter both cardiac and systemic metabolic substrate handling in mice.

© 2013 Elsevier Ltd. All rights reserved.

Address correspondence to Gary E. Shull, Department of Molecular Genetics, Biochemistry and Microbiology, University of Cincinnati College of Medicine, 231 Albert Sabin Way, Cincinnati, OH 45267-0524. shullge@ucmail.uc.edu, telephone: (513) 558-0056; Fax: (513) 558-1885.

Publisher's Disclaimer: This is a PDF file of an unedited manuscript that has been accepted for publication. As a service to our customers we are providing this early version of the manuscript. The manuscript will undergo copyediting, typesetting, and review of the resulting proof before it is published in its final citable form. Please note that during the production process errors may be discovered which could affect the content, and all legal disclaimers that apply to the journal pertain.

Disclosures

None.

Keywords

NHE-1; *Slc9a1*; metabolic syndrome; diabetes; insulin resistance

1. Introduction

The role of the NHE1 Na^+/H^+ exchanger (*Slc9a1*) in ischemia-reperfusion (I/R) injury and the benefits of NHE1 inhibition, as revealed by experimental studies, are well established [1–3]. Although short-term inhibition of NHE1 failed to improve patient outcomes in clinical trials [4–7], evidence from pre-clinical studies that chronic inhibition of NHE1 reduces post-infarction remodeling and heart failure indicates that long-term NHE1 inhibition might have protective effects [6,8–12]. The general consensus is that NHE1 inhibition protects against hypercontracture injury by attenuating Na^+ -loading, which in turn limits Ca^{2+} accumulation during ischemia [6]. However, recent *in vitro* studies have shown that NHE1 inhibition also protects mitochondrial integrity and reduces production of reactive oxygen species (ROS) [13–16]. This suggests that the cardioprotection resulting from NHE1 inhibition may also involve attenuation of oxidative stress, which is likely to be an important factor in the pathological conditions alleviated by NHE1 inhibition. There has, however, been no confirmation of the anti-oxidant effects of longterm NHE1 inhibition *in vivo*, nor is it known if NHE1 inhibition improves cardiac redox homeostasis under non-pathological conditions.

The purpose of the current study was to address these issues using the global NHE1-null mouse as a model of long-term NHE1 inhibition [17]. We previously reported that these mice are protected against acute I/R-induced myocardial injury [18]. Here we show that the long-term loss of NHE1 activity, which does not impair cardiovascular performance, leads to improved redox potential and substrate flexibility in heart, better preservation of insulin sensitivity, and appears to provide some protection against high-fat diet-induced myocardial stress. We also present evidence of systemic effects in NHE1-null mice that are consistent with the cardiac effects, with lower plasma glucose and insulin levels coupled with sharply reduced hepatic lipid accumulation upon exposure to a high-fat diet. These findings indicate that in addition to the therapeutic effects of short-term NHE1 inhibition on intracellular Na^+ and Ca^{2+} homeostasis, long-term inhibition may also have protective effects via enhanced antioxidant potential and impacts on metabolic substrate handling in both heart and extracardiac tissues.

2. Materials and Methods

2.1. Animals

Development and genotyping of global *Nhe1*^{-/-} mice were carried out as previously described [17]. Male and female mutant and wild-type (WT) mice of both a 129/SvJ and Black Swiss mixed background and an inbred FVB/N background (available from Jackson Labs; *Slc9a1*) were generated by breeding heterozygous mice. We reported previously that *Nhe1*^{-/-} mice exhibited growth retardation and a high incidence of sudden death from slow-wave epilepsy [17,18]. In the current study, by maintaining the mice in an isolated quiet room and handling them gently, growth was relatively normal, the incidence of spontaneous death was sharply reduced, and mutants were able to survive beyond one year of age. All procedures conformed to guidelines published by the National Institutes of Health (Guide for the Care and Use of Laboratory Animals; Publication No. 86–23, revised 1996) and were approved by the Institutional Animal Care and Use Committee at the University of Cincinnati.

2.2. Analysis of cardiovascular function in vivo

Adult mice were anesthetized with ketamine and inactin (50 and 100 µg/g bodyweight), and surgical preparation and analysis of cardiovascular performance were performed as described previously [19,20]. A PowerLab data-acquisition system (ADInstruments, Colorado Springs, CO) was used to record and analyze data.

2.3. Preparation of tissue samples for immunoblot and real-time PCR analyses

Mice were anesthetized with 2.5% Avertin (15 µl/g bodyweight) and allowed to stabilize for 10 min on a thermally controlled heating pad. Harvesting of hearts, preparation of total homogenates, myofibrillar and mitochondrial fractions, protein assays, and preparation and probing of immunoblots were performed as described previously [20–22]. Additional information about the antibodies used is provided in the supplementary data section.

Total RNA was isolated from cardiac samples and cDNA was synthesized using oligo dT primers as previously described [23]. Information about RNA Seq Analysis and about RT-PCR analysis and the primer sequences utilized is provided in the supplementary methods section.

2.4. GSH and GSSG levels

Both total and oxidized glutathione were determined using a Glutathione Assay kit (Cayman Chemical, Ann Arbor, MI). Frozen heart samples were processed according to the manufacturer's instructions to determine total (GSH + GSSG) and oxidized (GSSG) glutathione, and GSH levels were determined by subtracting oxidized from total glutathione.

2.5. High-fat diet and insulin treatment

Mice were placed on a high-fat diet (60% kcal fat content; catalog number D12492; Research Diets, Inc.) for the indicated periods of time. To determine changes in insulin signaling in heart, mice fed either normal chow or a high-fat diet were fasted for 2 hours immediately before administration of insulin (GIBCO). Hearts were harvested 30 minutes after insulin treatment (13.5 IU/kg bodyweight) and rapidly frozen in liquid nitrogen for future analysis.

2.6. Analysis of plasma

Blood was collected in the mid-afternoon (during the light cycle) from mice fasted for 2 hours and analyzed as previously described [24]. Levels of glucose, cholesterol, and nonesterified fatty acids (NEFA) were determined at the Mouse Metabolic Phenotyping Center, University of Cincinnati as described [24]. Insulin levels were determined by utilizing the services of Antech Diagnostics, Irvine, CA.

2.7. Microscopy and morphometry

Cardiac and hepatic (left lobe) tissues were fixed in 4% paraformaldehyde in phosphate buffer (pH 7.3) overnight and then post-fixed in 2% osmium tetroxide in phosphate buffer for 2 hours. Tissue was dehydrated, passed through two changes of 100% propylene oxide, Spurr's resin, embedded in fresh Spurr's resin, and cured at 60°C. Cardiac samples were subjected to electron microscopy (EM) morphometry, which was carried out at 10,000X magnification as described previously [25]. 1.5 µm thick plastic sections of liver samples were stained with toluidine blue and volume density of lipid droplets was obtained at 100X using a camera lucida to display the field upon a grid of 109 intersections. The intersections that fell over lipid droplets were counted and divided by the total number of intersections lying over cellular elements. Sampling of fields was random and genotype was not known by the operator.

2.8. Statistics

Values are presented as means \pm standard error (SE). One-way analysis of variance (ANOVA) and two-sided Student's t-test were used, and $P < 0.05$ was considered significant.

3. Results

3.1 Cardiovascular performance of NHE1-null mice in vivo

Cardiovascular performance under basal conditions and after β -adrenergic stimulation was analyzed in mice of both the mixed (129Svj and Blackswiss) background used for studies of IR injury [18], and an inbred FVB/N background (Fig. 1). Heart rates, mean arterial pressure and systolic left ventricular pressure did not differ significantly between *Nhe1*^{-/-} and WT mice of either background (data not shown). In the mixed background, contractility (Fig. 1A) and relaxation (Fig. 1C) were the same in both genotypes. In FVB/N mice, basal contractility (+dP/dt = 10675 \pm 306 in *Nhe1*^{-/-}, 8724 \pm 792 in WT; Fig. 1B) and relaxation (-dP/dt = -9733 \pm 470 in *Nhe1*^{-/-}, -7916 \pm 532 in WT; Fig. 1D) were significantly increased in NHE1-null mice. *Nhe1*^{-/-} mice of both backgrounds exhibited normal responses to β -adrenergic stimulation. All further analyses were carried out using mice of the FVB/N background.

3.2. Expression of transport mechanisms with potential for compensation

The lack of impairment of cardiovascular performance raised the possibility that other plasma membrane transport mechanisms mediating Na⁺-dependent alkalization provided some compensation for the loss of NHE1. RNA Seq analysis of mRNA from FVB/N WT hearts revealed very low expression of NHE3, NHE4, and NHE5 (RPKM values of 0.29 \pm 0.02; 0.44 \pm 0.06, and 0.64 \pm 0.06, respectively, compared with 9.10 \pm 0.20 for NHE1), which could be due to expression in cells other than myocytes. Transcript levels for NHE2 (*Slc9a2*) and for NHE8 (*Slc9a8*), which functions on the plasma membrane of major Na⁺-absorbing tissues [26,27], were 42% and 125% of NHE1 transcript levels, respectively (Fig. 2A). Expression of NBCe1 (*Slc4a4*) and NBCn1 (*Slc4a7*) Na⁺/HCO₃⁻ cotransporter mRNAs was 104% and 47% of NHE1 mRNA levels, respectively (Fig. 2A). RT-PCR analysis revealed no significant differences in mRNA expression for these transporters in NHE1-null hearts (Fig. 2B).

3.3 Alterations in Ca²⁺-handling proteins and troponin I in NHE1-null hearts

Increased basal contractility and relaxation, as seen in *Nhe1*^{-/-} mice of the FVB/N background, is often associated with changes in Ca²⁺-handling or myofibrillar proteins. Immunoblot analysis (Fig. 2C) confirmed that NHE1 was absent in *Nhe1*^{-/-} hearts. There were no significant changes in expression of the NCX1 Na⁺/Ca²⁺ exchanger (Fig. 2D) or L-type Ca²⁺ channel α 2 subunit (Fig. 2E). Unexpectedly, SERCA2a (Fig. 2F) expression was reduced to 82 \pm 6% of WT levels, while phospholamban (PLN) levels (Fig. 2G) were unaltered. Among myofibrillar proteins, we performed immunoblot analyses (Fig. 2H) for total and phosphorylated forms of troponin I (TnI) and myosin binding protein C (MyBP-C), which play important roles in the regulation of contractile function [28,29]. Expression of total TnI was slightly elevated in *Nhe1*^{-/-} hearts (Fig. 2I), but TnI phosphorylated on Ser23/24 (when normalized to total TnI, Fig. 2J), total MyBP-C (Fig. 2K), and MyBP-C phosphorylated on Ser282 (when normalized to total MyBP-C, Fig. 2L) were not altered.

3.4 Hearts of NHE1-null mice exhibit evidence of reduced oxidative stress

Oxidative stress plays a major role in heart disease [30,31], and treatment of cultured cells and tissue slices with NHE1 inhibitors reduces ROS production and oxidative stress [14,16].

To determine whether the redox state was altered in *Nhe1*^{-/-} hearts, we determined levels of reduced glutathione (GSH) and the ratio of reduced:oxidized glutathione (GSH:GSSG) in cardiac homogenates. GSH levels were increased by 55 ± 9% and the GSH:GSSG ratio was increased by 117 ± 22% in *Nhe1*^{-/-} hearts (Fig. 3A), indicating a more negative glutathione redox potential and a likely reduction in oxidative stress. Because reduced oxidative stress can result from enhanced expression of ROS scavenging enzymes, we examined levels of mitochondrial Mn superoxide dismutase (SOD2), cytosolic Cu/Zn superoxide dismutase (SOD1), and catalase (Fig. 3B). Expression of SOD2 was reduced to 79 ± 5% of WT levels in mitochondrial fractions of *Nhe1*^{-/-} hearts; expression of SOD1 and catalase were not altered. Thus, the apparent reduction in oxidative stress was not due to an increase in ROS scavenging enzymes.

The expression of heat shock proteins is strongly implicated in redox homeostasis [32]. Immunoblot analysis of stress-related proteins revealed reduced expression of heat shock proteins Hsp25/27 (83 ± 5% of WT) and Hsp60 (77 ± 5% of WT) in *Nhe1*^{-/-} hearts (Fig. 3C). In addition, mRNA levels of stress-related genes *Ankrd1* [33], encoding the cardiac ankyrin repeat protein (CARP, 77 ± 4% of WT) and *Ankrd23*, encoding the diabetes-related ankyrin repeat protein (DARP, 74 ± 4% of WT) were reduced in *Nhe1*^{-/-} hearts (Fig. 3D). The reduction in *Ankrd23* expression, which is upregulated in type 2 diabetes and insulin resistant muscle and has been shown to impair lipid uptake [34], is consistent with possible effects on metabolic substrate handling in *Nhe1*^{-/-} hearts.

3.5 Effects of loss of NHE1 on regulators of energy metabolism in heart

Mitochondrial function and the associated levels of ROS generation are intimately linked to changes in metabolic substrate utilization [35], which is in turn modulated by expression levels of sarcolemmal substrate transporters and mitochondrial enzymes [36]. Immunoblot analysis revealed that expression of glucose transporter 1 (GLUT1) was increased (Fig. 4A,B) in mutant hearts (137 ± 8% of WT levels), whereas expression of GLUT4 and fatty acid translocase FAT/CD36 were unaltered. Among the mitochondrial enzymes analyzed, PDK4, cytochrome C, and COX4 were not altered, but levels of 3-hydroxybutyrate dehydrogenase 1 (BDH1) were decreased (Fig. 4C,D) in mutant hearts (59 ± 4% of WT levels). Consistent with altered substrate handling, EM morphometric analysis revealed that the incidence of lipid droplets, indicative of lipid accumulation, was reduced in *Nhe1*^{-/-} hearts (Fig. 4E, 0.50 ± 0.14 lipid droplets/μm² in *Nhe1*^{-/-}; 2.73 ± 0.45 droplets/μm² in WT). Furthermore, mRNA levels for the transcriptional coactivators peroxisome proliferator-activated receptor coactivator 1α (PGC1α) and 1β (PGC1β), which are strongly implicated in the regulation of mitochondrial function, integrity and oxidative capacity [37,38], were increased in *Nhe1*^{-/-} hearts (Fig. 4F).

PDK4 inhibits the pyruvate dehydrogenase complex, thereby reducing the capacity for glucose oxidation [39,40], and is upregulated by a high fat diet [41]. To test the possibility that glucose utilization is better preserved in *Nhe1*^{-/-} hearts, we hypothesized that mutant hearts would be refractory to high-fat diet induced upregulation of PDK4. We analyzed cardiac homogenates from mice fed a high-fat diet for 10 days. While cardiac PDK4 levels increased by 46 ± 10% in WT mice on the high-fat diet, levels remained relatively constant in *Nhe1*^{-/-} hearts (-7 ± 7%) when compared to hearts from control mice on a normal diet (Fig. 5A,B). These results suggest that *Nhe1*^{-/-} hearts exhibit greater metabolic substrate flexibility, i.e., the ability to adjust substrate oxidation to substrate availability [42], when the mice are fed a high fat diet.

3.6 Protection against high-fat diet associated myocardial stress

Exposure to a high-fat diet is associated with the generation of ROS in heart [35]. Given the evidence of an improved antioxidant potential and altered substrate handling in *Nhe1*^{-/-} hearts, we investigated the possibility that *Nhe1*^{-/-} mice were protected against high-fat diet-induced myocardial stress. We determined levels of α B-crystallin phosphorylation on Ser59 (p- α B-crystallin) and Hsp25/27 phosphorylation on Ser82 (p-Hsp25/27), as evidence of oxidative stress [43,44], in cardiac homogenates from mice fed a high-fat diet for 10 days. WT hearts exhibited a greater increase in p- α B-crystallin (Fig. 6A,B, 210 \pm 10% in WT; 150 \pm 22% in *Nhe1*^{-/-}) and p-Hsp25/27 (Fig. 6A,C, 229 \pm 35% in WT; 97 \pm 13% in *Nhe1*^{-/-}), consistent with a reduction in high-fat diet induced myocardial stress in *Nhe1*^{-/-} hearts.

3.7 Evidence for attenuation of high-fat diet induced insulin resistance in *Nhe1*^{-/-} hearts

Reduced Hsp60 expression has been associated with insulin resistance and diabetes [45,46]. Insulin-signaling, however, as indicated by insulin-induced phosphorylation of PKB/Akt on Ser473 in hearts of WT and *Nhe1*^{-/-} mice fed a normal diet (Fig. 7A,B), was essentially the same in WT and mutant mice, with greater than 3-fold insulin stimulation of phosphorylation in both genotypes. Given the reduction in myocardial stress, we tested the hypothesis that mutant mice exhibited some degree of protection against high-fat diet-induced myocardial insulin resistance. This was done by determining levels of cardiac PKB/Akt phosphorylation upon acute administration of insulin to WT and *Nhe1*^{-/-} mice maintained on a high-fat diet for 8 weeks. The results (Fig. 7C,D) showed that stimulation of PKB/Akt phosphorylation was greater in *Nhe1*^{-/-} hearts (112 \pm 5% increase in *Nhe1*^{-/-} hearts *versus* 70 \pm 9% increase in WT hearts). These results indicate that *Nhe1*^{-/-} hearts are less susceptible to high-fat diet-induced insulin resistance than WT hearts, suggesting that reduced oxidative stress is responsible for the reduced Hsp60 levels.

3.8 Extracardiac effects of NHE1 ablation on serum glucose, insulin, and high-fat diet-induced hepatic lipid accumulation

Given the ubiquitous expression of NHE1, the findings in *Nhe1*^{-/-} hearts suggested that NHE1 ablation could have effects on systemic metabolic parameters and on other organs. Measurement of fasting plasma glucose, cholesterol, NEFA and insulin in mice fed a normal chow-diet revealed that while levels of cholesterol and NEFA were similar between the two genotypes, glucose (Fig. 8A, 80 \pm 13 mg/dL in *Nhe1*^{-/-}; 124 \pm 4 mg/dL in WT) and insulin (Fig. 8B, 8.8 \pm 0.4 μ U/mL in *Nhe1*^{-/-}; 10.5 \pm 0.6 μ U/mL in WT) were reduced in *Nhe1*^{-/-} mice. When placed on a high-fat diet for 8 weeks, bodyweight gain was blunted in *Nhe1*^{-/-} mice (Fig. 8C, 4.4 \pm 1.6 g in *Nhe1*^{-/-}; 9.6 \pm 1.9 g in WT) and glucose levels remained lower than in WT mice (Fig. 8D, 77 \pm 12 mg/dL in *Nhe1*^{-/-}; 115 \pm 4 mg/dL in WT). Plasma cholesterol and NEFA were similar in both genotypes (data not shown). Gross examination of livers from mice fed the high-fat diet suggested there was less lipid accumulation in *Nhe1*^{-/-} livers. Morphometric analysis revealed that the volume density of lipid droplets in *Nhe1*^{-/-} livers was reduced (Fig. 8E) and the lipid droplets tended to be smaller in *Nhe1*^{-/-} livers (Fig. 8F,G), indicating that high-fat diet induced hepatic lipid accumulation was reduced in *Nhe1*^{-/-} mice.

4. Discussion

Chronic inhibition of NHE1 is known to attenuate progression of cardiac hypertrophy and heart failure in animal models [8–12], and life-long treatment with cariporide caused a remarkable increase in lifespan of both hypertensive and normotensive rats, attenuating cardiac hypertrophy and fibrosis typically associated with aging [47]. Although there was a promising reduction in myocardial infarction following coronary artery bypass graft surgery [7], clinical trials using short-term inhibition of NHE1 have shown no overall therapeutic

benefit [4–7]. On the basis of results from animal studies, it has been suggested that long-term inhibition of NHE1 might be beneficial in some conditions [6]. In the current study, using the NHE1-null mouse line as a model of long-term NHE1 inhibition, we have shown that chronic loss of NHE1 activity does not impair cardiovascular performance and leads to metabolic changes in heart that may contribute to the cardioprotective effects associated with chronic NHE1 inhibition.

In addition to regulating intracellular pH, NHE1 mediates Na^+ uptake [48]. Therefore, ablation of NHE1 may reduce intracellular Na^+ and, in principle, could depress contractility by increasing NCX1-mediated Ca^{2+} -efflux. In *Nhe1*^{-/-} mice of the FVB/N background, however, contractility and relaxation, as measured by +dP/dt and -dP/dt, were slightly improved under basal conditions. This effect was dependent on background and was not observed in mice of the mixed 129Svj and Blackswiss background, which exhibited normal contractility and relaxation. Furthermore, while values of the relaxation time constant (τ), an alternative measure of relaxation [49], tended to be lower in *Nhe1*^{-/-} mice of the FVB/N background under basal conditions ($\tau = 10.40 \pm 0.45$ msec in *Nhe1*^{-/-}, 12.02 ± 0.95 msec in WT), consistent with improved relaxation, but the differences were not significant. The important point of these data is that the loss of NHE1 does not impair cardiovascular performance in mice under nonpathological conditions and, in some strains, might actually cause a slight improvement in function. Whether this is also true in humans is not known.

Given the reduction in SERCA2a levels, factors other than Ca^{2+} handling are likely to play a role in the preservation of cardiac function in NHE1-null mice. Given the evidence that oxidative stress can impair contractility [50], reduced oxidative stress is one possibility. A second possibility is that sufficient Na^+ -dependent alkalization can occur via other plasma membrane Na^+/H^+ exchangers or $\text{Na}^+/\text{HCO}_3^-$ cotransporters. The NBCn1 and NBCe1 $\text{Na}^+/\text{HCO}_3^-$ cotransporters are expressed in heart and, like NHE1, are induced during cardiac hypertrophy [51]; their combined transcript levels were greater than that of NHE1. NHE3, NHE4, and NHE5 were expressed at only low levels in heart, and it is possible that they are in cell types other than cardiomyocytes, such as fibroblasts, smooth muscle, endothelial cells, or nerve cells. NHE5 is a major neuronal isoform in brain, and there is evidence that NHE5 transcripts expressed in nonneuronal tissues are non-functional due to aberrant splicing [52], making it an unlikely myocyte isoform. NHE2 was detected previously at low levels in rat heart and at high levels in rat skeletal muscle [53]. In mouse heart, NHE2 mRNA levels were 42% of NHE1 levels. The biochemical properties of NHE1 and NHE2 differ, with NHE1 exhibiting a greater intracellular and extracellular sensitivity to H^+ [54]. It has been noted that the characteristics of Na^+/H^+ exchange in rat skeletal myotubes are consistent with the expression of both NHE1 and NHE2 [54,55]. Thus, it is possible that NHE2 could serve as a myocyte Na^+/H^+ exchanger. Surprisingly, NHE8 mRNA was more abundant in heart than NHE1 mRNA. NHE8 is expressed in intracellular membranes of many cells and on brush border plasma membranes of kidney and intestinal epithelial cells [26,27], where it plays a role in Na^+ absorption. Like NHE2, its cell-type distribution, membrane location, and function in heart have not been reported; however, given its relatively high expression levels it should be considered as a possible sarcolemmal/t-tubular Na^+/H^+ exchanger. None of these transporters were upregulated in *Nhe1*^{-/-} hearts; nevertheless, their combined activities may be sufficient to compensate for any deficit in Na^+ -dependent H^+ extrusion that might affect contractility.

The increases in GSH levels and GSH/GSSG ratios provide evidence that loss of NHE1 leads to a reduction in oxidative stress in *Nhe1*^{-/-} hearts. Reduced oxidative stress can result from augmented ROS scavenging mechanisms or reduced ROS production. Several ROS scavenging enzymes contribute to the antioxidant defenses of cardiac myocytes, and overexpression of SOD2 has been shown to be protective [56]. However, expression of

SOD2 was down-regulated in *Nhe1*^{-/-} hearts, suggesting that mitochondrial ROS production was reduced. Although reduced Hsp60 expression has been associated with insulin resistance and diabetes [45,46], insulin signaling was normal in *Nhe1*^{-/-} hearts when the mice were fed a normal diet and was higher than that of WT hearts when fed a high-fat diet. Oxidative stress also impacts heat shock proteins [32]; therefore, the lower levels of Hsp60 and Hsp25/27 are a likely consequence of the improved redox status in *Nhe1*^{-/-} hearts. These results are consistent with studies showing that treatment with NHE1 inhibitors reduces mitochondrial ROS production [14–16]. The mechanism is unclear but there is evidence that anti-ROS effects of NHE1 inhibitors are caused by inhibition of mitochondrial Na⁺/H⁺ exchange [57], and recent data suggest that NHE1 is also expressed in the mitochondrial inner membrane [58,59].

Mitochondrial ROS generation is affected by changes in metabolic substrate utilization [35,36]. Although the heart can metabolize many substrates, it utilizes both long-chain fatty acids and glucose as major metabolic substrates. Substrate flexibility in cardiac myocytes is modulated in part by sarcolemmal transporters regulating the uptake of metabolic substrates [60]. GLUT1 overexpression in heart has been shown to increase glucose uptake and glycolysis [61], and in response to a high-fat diet, leads to increased oxidative stress and reduced metabolic substrate flexibility [62]. Increased GLUT1 in *Nhe1*^{-/-} hearts likely reflects higher glucose utilization and it is possible that this could exacerbate high-fat diet-induced oxidative stress. However, GLUT1 levels in *Nhe1*^{-/-} mice were much lower than in the GLUT1 overexpression studies [61,62], and the reduction in high-fat diet-induced stimulation of α B-crystallin and Hsp25/27 phosphorylation suggests that it does not increase oxidative stress. Also, the reduced incidence of lipid droplets in *Nhe1*^{-/-} myocardium and the increased expression of mRNAs encoding PGC1 α and PGC1 β , which promote fatty acid metabolism [37,38], were consistent with a phenotype in which lipid metabolism was not impaired. Efficient oxidation of both fatty acids and glucose are necessary for optimal cardiac energy metabolism and imbalances in substrate utilization or reduced glucose oxidation can contribute to heart disease [63]. Therefore, the cardioprotective effects of chronic NHE1 inhibition may involve increased glucose utilization under conditions in which it might normally be suppressed.

To obtain beneficial effects from increased glucose metabolism, glycolysis must be efficiently coupled with pyruvate oxidation. This critical step in carbohydrate metabolism is catalyzed by the pyruvate dehydrogenase complex (PDH), which is negatively regulated by the PDK family of kinases. A sustained increase in lipid delivery to the heart leads to upregulation of PDK4, which reduces glucose oxidation [64]. We found that, in contrast to WT controls, PDK4 protein expression in *Nhe1*^{-/-} hearts was resistant to high-fat diet-induced upregulation. Loss of PDK4 expression has been shown to alleviate high-fat diet-induced suppression of PDH activity [65]. Therefore, under conditions of increased lipid utilization, PDK4-mediated uncoupling of glycolysis from pyruvate oxidation is likely to be attenuated in *Nhe1*^{-/-} hearts. These results suggest that chronic inhibition of NHE1 may reduce mitochondrial ROS generation in part by preserving metabolic substrate flexibility.

Oxidative stress and lipotoxicity have been implicated in the development of high-fat diet-induced insulin resistance [35,36,66]. The attenuation of high-fat diet induced myocardial stress raised the possibility that insulin signaling was better preserved in *Nhe1*^{-/-} hearts. However, given the finding that PDK4 expression in *Nhe1*^{-/-} hearts was resistant to high-fat diet-induced upregulation, it seemed possible that mutant hearts might be more susceptible to insulin resistance upon chronic high-fat feeding. While chronic exposure to a high-fat diet depressed insulin signaling in both WT and mutant hearts, we found significantly greater preservation of insulin signaling in *Nhe1*^{-/-} hearts, as indicated by insulin-induced phosphorylation of PKB/Akt [67]. These results suggest that development of insulin

resistance is attenuated in *Nhe1*^{-/-} hearts, possibly due to their improved antioxidant potential. Interestingly, it has been shown that insulin-induced stimulation of PKB/Akt protects cardiomyocytes against oxidative stress [68], that some of the Akt phosphorylated in response to insulin translocates to mitochondria [69], and that phosphorylation by PKB/Akt inhibits NHE1 [70]. Thus, it is possible that some of the cardioprotective effects of insulin stimulation are due to the inhibition of NHE1 and that genetic ablation of NHE1 or inhibition with drugs such as cariporide mimic this action.

Given the metabolic changes in hearts of the global NHE1-null mouse and the cardioprotection observed during ischemia-reperfusion (IR) injury in both isolated hearts treated with NHE1 inhibitors and in NHE1-null hearts [3,18], it is interesting that a mouse model with cardiomyocyte-specific overexpression of activated NHE1 exhibits altered metabolism and cardioprotection in IR injury [71]. The isolated hearts used in that study had increased fatty acid oxidation and glycolysis, but appeared to have both reduced glucose oxidation and uncoupling of glycolysis and glucose oxidation. These mice and another mouse model of cardiac-specific overexpression of an activated NHE1 develop severe hypertrophy and heart failure [72,73], consistent with the observations that long-term inhibition of NHE1 activity, rather than enhanced activity, is cardioprotective with respect to hypertrophy and heart failure [1,8–11].

During treatment of mice with the high-fat diet, we were surprised to see that *Nhe1*^{-/-} mice did not develop fatty livers, which were very apparent in WT mice upon visual inspection. Histological analyses confirmed that lipid deposition was significantly less in *Nhe1*^{-/-} livers than in WT controls, suggesting that loss of NHE1 has a major effect on liver metabolism. This observation and the reduction in plasma glucose and insulin suggest that some of the beneficial effects of long-term NHE1 inhibition on cardiovascular disease might be due to metabolic effects in extracardiac tissues. The liver plays a central role in metabolism, and non-alcoholic fatty liver disease (NAFLD) is the most common liver disease in the western world. NAFLD is closely associated with obesity and metabolic syndrome, and it is a major cardiovascular risk factor, with effects on insulin resistance, deposition of visceral and epicardial fat, systemic inflammation, and dyslipidemia [74,75]. The NHE1 inhibitor cariporide has been shown to reduce liver fibrosis in rats and this was accompanied by reduced activation of hepatic stellate cells [76], a major cell type involved in NAFLD [77]. Thus, one could speculate that NHE1 inhibitors might be useful in the treatment of NAFLD, although it should be noted that the lipid deposition we observed was in hepatocytes and stellate cells did not appear to be affected.

In summary, our studies demonstrate that the loss of NHE1 in otherwise healthy mice does not impair cardiovascular function, and leads to metabolic changes that are consistent with the known cardioprotective effects of NHE1 inhibition. The antioxidant potential of the heart was enhanced, high-fat diet-induced myocardial stress and insulin-resistance were attenuated, plasma glucose and insulin were reduced, and the mice were surprisingly resistant to increased lipid deposition in liver when fed a high-fat diet. PDK4 expression was resistant to high-fat diet-induced upregulation in *Nhe1*^{-/-} hearts, suggesting that metabolic substrate flexibility is enhanced in *Nhe1*^{-/-} hearts under conditions of a high-fat diet. An intriguing question that emerges from these observations is whether inhibition of NHE1 leads to enhanced insulin sensitivity in pathological conditions such as hyperthyroidism, diabetes, metabolic syndrome, and fatty liver disease. A number of *in vivo* studies of the effects of NHE1 inhibition on other tissues suggest that these inhibitors have such an effect. In diabetic rodent models, cariporide improved insulin sensitivity in an insulin-resistant rat [78], and in other diabetic models it led to reductions in both vascular hypertrophy and in cataracts and oxidative stress in the retina [79,80]. It is possible that some of the newer

NHE1 inhibitors, which are being developed for chronic dosing [81], will be suitable for treatment of heart disease and metabolic conditions that affect other organs as well.

Supplementary Material

Refer to Web version on PubMed Central for supplementary material.

Acknowledgments

This study was supported by NIH grants HL061974 and DK050594. VP was partially supported by American Heart Association 11BGIA7720005. MLM was supported by P30ES006096 (Center for Environmental Genetics). The Mouse Metabolic Phenotyping Center is supported by a U24 grant DK059630. We thank Maureen Bender for excellent animal husbandry.

References

1. Karmazyn M, Kili A, Javadov S. The role of NHE-1 in myocardial hypertrophy and remodelling. *J Mol Cell Cardiol.* 2008; 44:647–653. [PubMed: 18329039]
2. Gumina RJ, Buerger E, Eickmeier C, Moore J, Daemmgen J, Gross GJ. Inhibition of Na⁺/H⁺ exchanger confers greater cardioprotection against 90 minutes of myocardial ischemia than ischemic preconditioning in dogs. *Circulation.* 1999; 100:2519–2526. [PubMed: 10604890]
3. Stromer H, de Groot MC, Horn M, Faul C, Leupold A, Morgan JP, et al. Na⁺/H⁺ exchange inhibition with HOE642 improves postischemic recovery due to attenuation of Ca²⁺ overload and prolonged acidosis on reperfusion. *Circulation.* 2000; 101:2749–2755. [PubMed: 10851214]
4. Theroux P, Chaitman BR, Danchin N, Erhardt L, Meinertz T, Schroeder JS, et al. Inhibition of the sodium-hydrogen exchanger with cariporide to prevent myocardial infarction in high-risk ischemic situations. Main results of the GUARDIAN trial. Guard during ischemia against necrosis (GUARDIAN) investigators. *Circulation.* 2000; 102:3032–3038. [PubMed: 11120691]
5. Zeymer U, Suryapranata H, Monassier JP, Opolski G, Davies J, Rasmanis G, et al. ESCAMI Investigators. The Na⁺/H⁺ exchange inhibitor eniporide as an adjunct to early reperfusion therapy for acute myocardial infarction. Results of the evaluation of the safety and cardioprotective effects of eniporide in acute myocardial infarction (ESCAMI) trial. *J Am Coll Cardiol.* 2001; 38:1644–1650. [PubMed: 11704395]
6. Avkiran M, Marber MS. Na⁺/H⁺ exchange inhibitors for cardioprotective therapy: progress, problems and prospects. *J Am Coll Cardiol.* 2002; 39:747–753. [PubMed: 11869836]
7. Mentzer RM, Bartels C, Bolli R, Boyce S, Buckberg GD, Chaitman B, et al. Sodiumhydrogen exchange inhibition by cariporide to reduce the risk of ischemic cardiac events in patients undergoing coronary artery bypass grafting: results of the EXPEDITION study. *Ann Thorac Surg.* 2008; 85:1261–1270. [PubMed: 18355507]
8. Baartscheer A. Chronic inhibition of Na⁺/H⁺-exchanger in the heart. *Curr Vasc Pharmacol.* 2006; 4:23–29. [PubMed: 16472174]
9. Yoshida H, Karmazyn M. Na⁺/H⁺ exchange inhibition attenuates hypertrophy and heart failure in 1-wk postinfarction rat myocardium. *Am J Physiol Heart Circ Physiol.* 2000; 278:H300–H304. [PubMed: 10644613]
10. Engelhardt S, Hein L, Keller U, Klambt K, Lohse MJ. Inhibition of Na⁺/H⁺ exchange prevents hypertrophy, fibrosis, and heart failure in β1-adrenergic receptor transgenic mice. *Circ Res.* 2002; 90:814–819. [PubMed: 11964375]
11. Baartscheer A, Hardziyenka M, Schumacher CA, Belterman CNW, van Borren MMGJ, Verkerk AO, et al. Chronic inhibition of the Na⁺/H⁺-exchanger causes regression of hypertrophy, heart failure, and ionic and electrophysiological remodelling. *Br J Pharmacol.* 2008; 154:1266–1275. [PubMed: 18493245]
12. Darmellah A, Baetz D, Prunier F, Tamareille S, Rucker-Martin C, Feuvray D. Enhanced activity of the myocardial Na⁺/H⁺ exchanger contributes to left ventricular hypertrophy in the Goto-Kakizaki rat model of type 2 diabetes: critical role of Akt. *Diabetologia.* 2007; 50:1335–1344. [PubMed: 17429605]

13. Teshima Y, Akao M, Jones SP, Marban E. Cariporide (HOE642), a selective Na^+/H^+ exchange inhibitor, inhibits the mitochondrial death pathway. *Circulation*. 2003; 108:2275–2281. [PubMed: 14568900]
14. Javadov S, Baetz D, Rajapurohitam V, Zeidan A, Kirshenbaum LA, Karmazyn M. Antihypertrophic effect of Na^+/H^+ exchanger isoform 1 inhibition is mediated by reduced mitogen-activated protein kinase activation secondary to improved mitochondrial integrity and decreased generation of mitochondrial-derived reactive oxygen species. *J Pharmacol Exp Ther*. 2006; 317:1036–1043. [PubMed: 16513848]
15. Toda T, Kadono T, Hoshiai M, Eguchi Y, Nakazawa S, Nakazawa H, et al. Na^+/H^+ exchanger inhibitor cariporide attenuates the mitochondrial Ca^{2+} overload and PTP opening. *Am J Physiol Heart Circ Physiol*. 2007; 293:H3517–H3523. [PubMed: 17906113]
16. Garciarena CD, Caldiz CI, Correa MV, Schinella GR, Mosca SM, Chiappe de Cingolani GE, et al. Na^+/H^+ exchanger-1 inhibitors decrease myocardial superoxide production via direct mitochondrial action. *J Appl Physiol*. 2008; 105:1706–1713. [PubMed: 18801963]
17. Bell SM, Schreiner CM, Schultheis PJ, Miller ML, Evans RL, Vorhees CV, et al. Targeted disruption of the murine *Nhe1* locus induces ataxia, growth retardation, and seizures. *Am J Physiol*. 1999; 276:C788–C795. [PubMed: 10199808]
18. Wang Y, Meyer JW, Ashraf M, Shull GE. Mice with a null mutation in the *NHE1* Na^+/H^+ exchanger are resistant to cardiac ischemia-reperfusion injury. *Circ Res*. 2003; 93:776–782. [PubMed: 12970112]
19. Lorenz JN, Robbins J. Measurement of intraventricular pressure and cardiac performance in the intact closed-chest anesthetized mouse. *Am J Physiol*. 1997; 272:H1137–H1146. [PubMed: 9087586]
20. Prasad V, Bodi I, Meyer JW, Wang Y, Ashraf M, Engle SJ, et al. Impaired cardiac contractility in mice lacking both the *AE3* $\text{Cl}^-/\text{HCO}_3^-$ exchanger and the *NKCC1* $\text{Na}^+/\text{K}^+/\text{2Cl}^-$ cotransporter: effects on Ca^{2+} handling and protein phosphatases. *J Biol Chem*. 2008; 283:31303–31314. [PubMed: 18779325]
21. Golenhofen N, Ness W, Koob R, Htun P, Schaper W, Drenckhahn D. Ischemia-induced phosphorylation and translocation of stress protein alpha B-crystallin to Z lines of myocardium. *Am J Physiol*. 1998; 274:H1457–H1464. [PubMed: 9612350]
22. Jin JK, Whittaker R, Glassy MS, Barlow SB, Gottlieb RA, Glembotski CC. Localization of phosphorylated alphaB-crystallin to heart mitochondria during ischemia-reperfusion. *Am J Physiol Heart Circ Physiol*. 2008; 294:H337–H344. [PubMed: 17993600]
23. Al Moamen NJ, Prasad V, Bodi I, Miller ML, Neiman ML, Lasko VM, et al. Loss of the *AE3* anion exchanger in a hypertrophic cardiomyopathy model causes rapid decompensation and heart failure. *J Mol Cell Cardiol*. 2011; 50:137–146. [PubMed: 21056571]
24. Bradford EM, Miller ML, Prasad V, Nieman ML, Gawenis LR, Berryman M, et al. *CLIC5* mutant mice are resistant to diet-induced obesity and exhibit gastric hemorrhaging and increased susceptibility to torpor. *Am J Physiol Regul Integr Comp Physiol*. 2010; 298:R1531–R1542. [PubMed: 20357015]
25. Miller ML, Andringa A, Zavros Y, Bradford EM, Shull GE. Volume density, distribution, and ultrastructure of secretory and basolateral membranes and mitochondria predict parietal cell secretory (dys)function. *J Biomed Biotechnol*. 2010; 2010:394198. [PubMed: 20339514]
26. Wang C, Xu H, Chen H, Li J, Zhang B, Tang C, et al. Somatostatin stimulates intestinal *NHE8* expression via p38 MAPK pathway. *Am J Physiol Cell Physiol*. 2011; 300:C375–C382. [PubMed: 21106692]
27. Baum M, Twombly K, Gattineni J, Joseph C, Wang L, Zhang Q, et al. Proximal tubule Na^+/H^+ exchanger activity in adult *NHE8*^{-/-}, *NHE3*^{-/-}, and *NHE3*^{-/-}/*NHE8*^{-/-} mice. *Am J Physiol Renal Physiol*. 2012; 303:F1495–F1502. [PubMed: 23054255]
28. Layland J, Solaro RJ, Shah AM. Regulation of cardiac contractile function by troponin I phosphorylation. *Cardiovasc Res*. 2005; 66:12–21. [PubMed: 15769444]
29. Barefield D, Sadayappan S. Phosphorylation and function of cardiac myosin binding protein-C in health and disease. *J Mol Cell Cardiol*. 2010; 48:866–875. [PubMed: 19962384]

30. Maack C, Böhm M. Targeting mitochondrial oxidative stress in heart failure throttling the afterburner. *J Am Coll Cardiol.* 2011; 58:83–86. [PubMed: 21620605]
31. Tsutsui H, Kinugawa S, Matsushima S. Oxidative stress and heart failure. *Am J Physiol Heart Circ Physiol.* 2011; 301:H2181–H2190. [PubMed: 21949114]
32. Christians ES, Ishiwata T, Benjamin IJ. Small heat shock proteins in redox metabolism: implications for cardiovascular diseases. *Int J Biochem Cell Biol.* 2012; 44:1632–1645. [PubMed: 22710345]
33. Mikhailov AT, Torrado M. The enigmatic role of the ankyrin repeat domain 1 gene in heart development and disease. *Int J Dev Biol.* 2008; 52:811–821. [PubMed: 18956313]
34. Ikeda K, Emoto N, Matsuo M, Yokoyama M. Molecular identification and characterization of a novel nuclear protein whose expression is up-regulated in insulin-resistant animals. *J Biol Chem.* 2003; 278:3514–3520. [PubMed: 12456686]
35. Dirx E, Schwenk RW, Glatz JF, Luiken JJ, van Eys GJ. High fat diet induced diabetic cardiomyopathy. *Prostaglandins Leukot Essent Fatty Acids.* 2011; 85:219–225. [PubMed: 21571515]
36. Stanley WC, Recchia FA, Lopaschuk GD. Myocardial substrate metabolism in the normal and failing heart. *Physiol Rev.* 2005; 85:1093–1129. [PubMed: 15987803]
37. Patti ME, Butte AJ, Crunkhorn S, Cusi K, Berria R, Kashyap S, et al. Coordinated reduction of genes of oxidative metabolism in humans with insulin resistance and diabetes: Potential role of PGC1 and NRF1. *Proc Natl Acad Sci U S A.* 2003; 100:8466–8471. [PubMed: 12832613]
38. Riehle C, Abel ED. PGC-1 proteins and heart failure. *Trends Cardiovasc Med.* 2012; 22:98–105. [PubMed: 22939990]
39. Chambers KT, Leone TC, Sambandam N, Kovacs A, Wagg CS, Lopaschuk GD, et al. Chronic inhibition of pyruvate dehydrogenase in heart triggers an adaptive metabolic response. *J Biol Chem.* 2011; 286:11155–11162. [PubMed: 21321124]
40. Hwang B, Jeoung NH, Harris RA. Pyruvate dehydrogenase kinase isoenzyme 4 (PDHK4) deficiency attenuates the long-term negative effects of a high-saturated fat diet. *Biochem J.* 2009; 423:243–252. [PubMed: 19627255]
41. Zhang L, Mori J, Wagg C, Lopaschuk GD. Activating cardiac E2F1 induces up-regulation of pyruvate dehydrogenase kinase 4 in mice on a short term of high fat feeding. *FEBS Lett.* 2012; 586:996–1003. [PubMed: 22569253]
42. Galgani JE, Moro C, Ravussin E. Metabolic flexibility and insulin resistance. *Am J Physiol Endocrinol Metab.* 2008; 295:E1009–E1017. [PubMed: 18765680]
43. Aggeli IK, Beis I, Gaitanaki C. Oxidative stress and calpain inhibition induce alpha B-crystallin phosphorylation via p38-MAPK and calcium signalling pathways in H9c2 cells. *Cell Signal.* 2008; 20:1292–1302. [PubMed: 18420382]
44. Clerk A, Michael A, Sugden PH. Stimulation of multiple mitogen-activated protein kinase sub-families by oxidative stress and phosphorylation of the small heat shock protein, HSP25/27, in neonatal ventricular myocytes. *Biochem J.* 1998; 333:581–589. [PubMed: 9677316]
45. Hooper PL. Insulin signaling, GSK-3, heat shock proteins and the natural history of type 2 diabetes mellitus: a hypothesis. *Metab Syndr Relat Disord.* 2007; 5:220–230. [PubMed: 18370776]
46. Chen H-S, Wu T-E, Juan C-C, Lin H-D. Myocardial heat shock protein 60 expression in insulin-resistant and diabetic rats. *J Endocrinol.* 2009; 200:151–157. [PubMed: 18948349]
47. Linz WJ, Busch AE. NHE-1 inhibition: from protection during acute ischaemia/reperfusion to prevention/reversal of myocardial remodeling. *Naunyn Schmiedebergs Arch Pharmacol.* 2003; 368:239–246. [PubMed: 14504689]
48. Bers DM, Barry WH, Despa S. Intracellular Na⁺ regulation in cardiac myocytes. *Cardiovasc Res.* 2003; 57:897–912. [PubMed: 12650868]
49. Weiss JL, Frederiksen JW, Weisfeldt ML. Hemodynamic determinants of the time-course of fall in canine left ventricular pressure. *J Clin Invest.* 1976; 58:751–760. [PubMed: 956400]
50. Bayeva M, Ardehali H. Mitochondrial dysfunction and oxidative damage to sarcomeric proteins. *Curr Hypertens Rep.* 2010; 12:426–432. [PubMed: 20865351]

51. Yamamoto T, Shirayama T, Sakatani T, Takahashi T, Tanaka H, Takamatsu T, et al. Enhanced activity of ventricular $\text{Na}^+ - \text{HCO}_3^-$ cotransport in pressure overload hypertrophy. *Am J Physiol Heart Circ Physiol*. 2007; 293:H1254–H1264. [PubMed: 17416604]
52. Baird NR, Orłowski J, Szabó EZ, Zaun HC, Schultheis PJ, Menon AG, et al. Molecular cloning, genomic organization, and functional expression of Na^+/H^+ exchanger isoform 5 (NHE5) from human brain. *J Biol Chem*. 1999; 274:4377–4382. [PubMed: 9933641]
53. Wang Z, Orłowski J, Shull GE. Primary structure and functional expression of a novel gastrointestinal isoform of the rat Na/H exchanger. *J Biol Chem*. 1993; 268:11925–11928. [PubMed: 7685026]
54. Yu FH, Shull GE, Orłowski J. Functional properties of the rat Na/H exchanger NHE-2 isoform expressed in Na/H exchanger-deficient Chinese hamster ovary cells. *J Biol Chem*. 1993; 268:25536–25541. [PubMed: 8244989]
55. Vigne P, Frelin C, Lazdunski M. The Na^+/H^+ antiport is activated by serum and phorbol esters in proliferating myoblasts but not in differentiated myotubes. Properties of the activation process. *J Biol Chem*. 1985; 260:8008–8013. [PubMed: 2989272]
56. Shen X, Zheng S, Metreveli NS, Epstein PN. Protection of cardiac mitochondria by overexpression of MnSOD reduced diabetic cardiomyopathy. *Diabetes*. 2006; 55:798–805. [PubMed: 16505246]
57. Ruiz-Meana M, Garcia-Dorado D, Pina P, Inseste J, Agulló L, Soler-Soler J. Cariporide preserves mitochondrial proton gradient and delays ATP depletion in cardiomyocytes during ischemic conditions. *Am J Physiol Heart Circ Physiol*. 2003; 285:H999–H1006. [PubMed: 12915386]
58. Javadov S, Rajapurohitam V, Kili A, Hunter JC, Zeidan A, Said Faruq N, et al. Expression of mitochondrial fusion-fission proteins during post-infarction remodeling: the effect of NHE-1 inhibition. *Basic Res Cardiol*. 2011; 106:99–109. [PubMed: 20886221]
59. Villa-Abrille MC, Cingolani E, Cingolani HE, Alvarez BV. Silencing of cardiac mitochondrial NHE1 prevents mitochondrial permeability transition pore opening. *Am J Physiol Heart Circ Physiol*. 2011; 300:H1237–H1251. [PubMed: 21297023]
60. Glatz JFC, Bonen A, Ouwens DM, Luiken JJFP. Regulation of sarcolemmal transport of substrates in the healthy and diseased heart. *Cardiovasc Drugs Ther*. 2006; 20:471–476. [PubMed: 17119873]
61. Liao R, Jain M, Cui L, D'Agostino J, Aiello F, Luptak I, et al. Cardiac-specific overexpression of GLUT1 prevents the development of heart failure attributable to pressure overload in mice. *Circulation*. 2002; 106:2125–2131. [PubMed: 12379584]
62. Yan J, Young ME, Cui L, Lopaschuk GD, Liao R, Tian R. Increased glucose uptake and oxidation in mouse hearts prevent high fatty acid oxidation but cause cardiac dysfunction in diet-induced obesity. *Circulation*. 2009; 119:2818–2828. [PubMed: 19451348]
63. Jaswal JS, Keung W, Wang W, Ussher JR, Lopaschuk GD. Targeting fatty acid and carbohydrate oxidation--a novel therapeutic intervention in the ischemic and failing heart. *Biochim Biophys Acta*. 2011; 1813:1333–1350. [PubMed: 21256164]
64. Sugden MC. PDC deletion: the way to a man's heart disease. *Am J Physiol Heart Circ Physiol*. 2008; 295:H917–H919. [PubMed: 18641270]
65. Jeoung NH, Harris RA. Pyruvate dehydrogenase kinase-4 deficiency lowers blood glucose and improves glucose tolerance in diet-induced obese mice. *Am J Physiol Endocrinol Metab*. 2008; 295:E46–E54. [PubMed: 18430968]
66. Kim JA, Wei Y, Sowers JR. Role of mitochondrial dysfunction in insulin resistance. *Circ Res*. 2008; 102:401–414. [PubMed: 18309108]
67. Yu W, Chen C, Fu Y, Wang X, Wang W. Insulin signaling: a possible pathogenesis of cardiac hypertrophy. *Cardiovasc Ther*. 2010; 28:101–105. [PubMed: 20398099]
68. Aikawa R, Nawano M, Gu Y, Katagiri H, Asano T, Zhu W, et al. Insulin prevents cardiomyocytes from oxidative stress-induced apoptosis through activation of PI3 kinase/Akt. *Circulation*. 2000; 102:2873–2879. [PubMed: 11104747]
69. Su CC, Yang JY, Leu HB, Chen Y, Wang PH. Mitochondrial Akt-regulated mitochondrial apoptosis signaling in cardiac muscle cells. *Am J Physiol Heart Circ Physiol*. 2012; 302:H716–H723. [PubMed: 22081709]

70. Snabaitis AK, Cuello F, Avkiran M. Protein kinase B/Akt phosphorylates and inhibits the cardiac Na^+/H^+ exchanger NHE1. *Circ Res.* 2008; 103:881–890. [PubMed: 18757828]
71. Mraiche F, Wagg CS, Lopaschuk GD, Fliegel L. Elevated levels of activated NHE1 protect the myocardium and improve metabolism following ischemia/reperfusion injury. *J Mol Cell Cardiol.* 2011; 50:157–164. [PubMed: 20974148]
72. Mraiche F, Oka T, Gan XT, Karmazyn M, Fliegel L. Activated NHE1 is required to induce early cardiac hypertrophy in mice. *Basic Res Cardiol.* 2011; 106:603–616. [PubMed: 21359875]
73. Nakamura TY, Iwata Y, Arai Y, Komamura K, Wakabayashi S. Activation of Na^+/H^+ exchanger 1 is sufficient to generate Ca^{2+} signals that induce cardiac hypertrophy and heart failure. *Circ Res.* 2008; 103:891–899. [PubMed: 18776042]
74. Bhatia LS, Curzen NP, Calder PC, Byrne CD. Non-alcoholic fatty liver disease: a new and important cardiovascular risk factor? *Eur Heart J.* 2012; 33:1190–1200. [PubMed: 22408036]
75. Gaggini M, Morelli M, Buzzigoli E, DeFronzo RA, Bugianesi E, Gastaldelli A. Nonalcoholic fatty liver disease (NAFLD) and its connection with insulin resistance, dyslipidemia, atherosclerosis and coronary heart disease. *Nutrients.* 2013; 5:1544–1560. [PubMed: 23666091]
76. Di Sario A, Bendia E, Taffetani S, Marzoni M, Candelaresi C, Pignini P, et al. Selective Na^+/H^+ exchange inhibition by cariporide reduces liver fibrosis in the rat. *Hepatology.* 2003; 37:256–266. [PubMed: 12540775]
77. Vanni E, Bugianesi E, Kotronen A, De Minicis S, Yki-Järvinen H, Svegliati-Baroni G. From the metabolic syndrome to NAFLD or vice versa? *Dig Liver Dis.* 2010; 42:320–330. [PubMed: 20207596]
78. Russell JC, Proctor SD, Kelly SE, Löhn M, Busch AE, Schäfer S. Insulin-sensitizing and cardiovascular effects of the sodium-hydrogen exchange inhibitor, cariporide, in the JCR: LA-cp rat and db/db mouse. *J Cardiovasc Pharmacol.* 2005; 46:746–753. [PubMed: 16306797]
79. Jandeleit-Dahm K, Hannan KM, Farrelly CA, Allen TJ, Rumble JR, Gilbert RE, et al. Diabetes-induced vascular hypertrophy is accompanied by activation of Na^+/H^+ exchange and prevented by Na^+/H^+ exchange inhibition. *Circ Res.* 2000; 87:1133–1140. [PubMed: 11110770]
80. Lupachyk S, Stavniichuk R, Komissarenko JI, Drel VR, Obrosova AA, El-Remessy AB, et al. Na^+/H^+ -exchanger-1 inhibition counteracts diabetic cataract formation and retinal oxidative-nitrative stress and apoptosis. *Int J Mol Med.* 2012; 29:989–998. [PubMed: 22407349]
81. Huber JD, Bentzien J, Boyer SJ, Burke J, De Lombaert S, Eickmeier C, et al. Identification of a potent sodium hydrogen exchanger isoform 1 (NHE1) inhibitor with a suitable profile for chronic dosing and demonstrated cardioprotective effects in a preclinical model of myocardial infarction in the rat. *J Med Chem.* 2012; 55:7114–7140. [PubMed: 22803959]

Highlights

- ▶ Cardiac function is not impaired by global genetic ablation of NHE1 Na/H exchanger
- ▶ GSH levels and GSH:GSSG ratios in NHE1-null hearts indicate enhanced redox potential
- ▶ NHE1-null hearts are protected against high-fat diet-induced myocardial stress
- ▶ Insulin sensitivity in response to high-fat is better preserved in NHE1-null hearts
- ▶ High-fat diet-induced hepatic lipid accumulation is reduced in NHE1-null mice

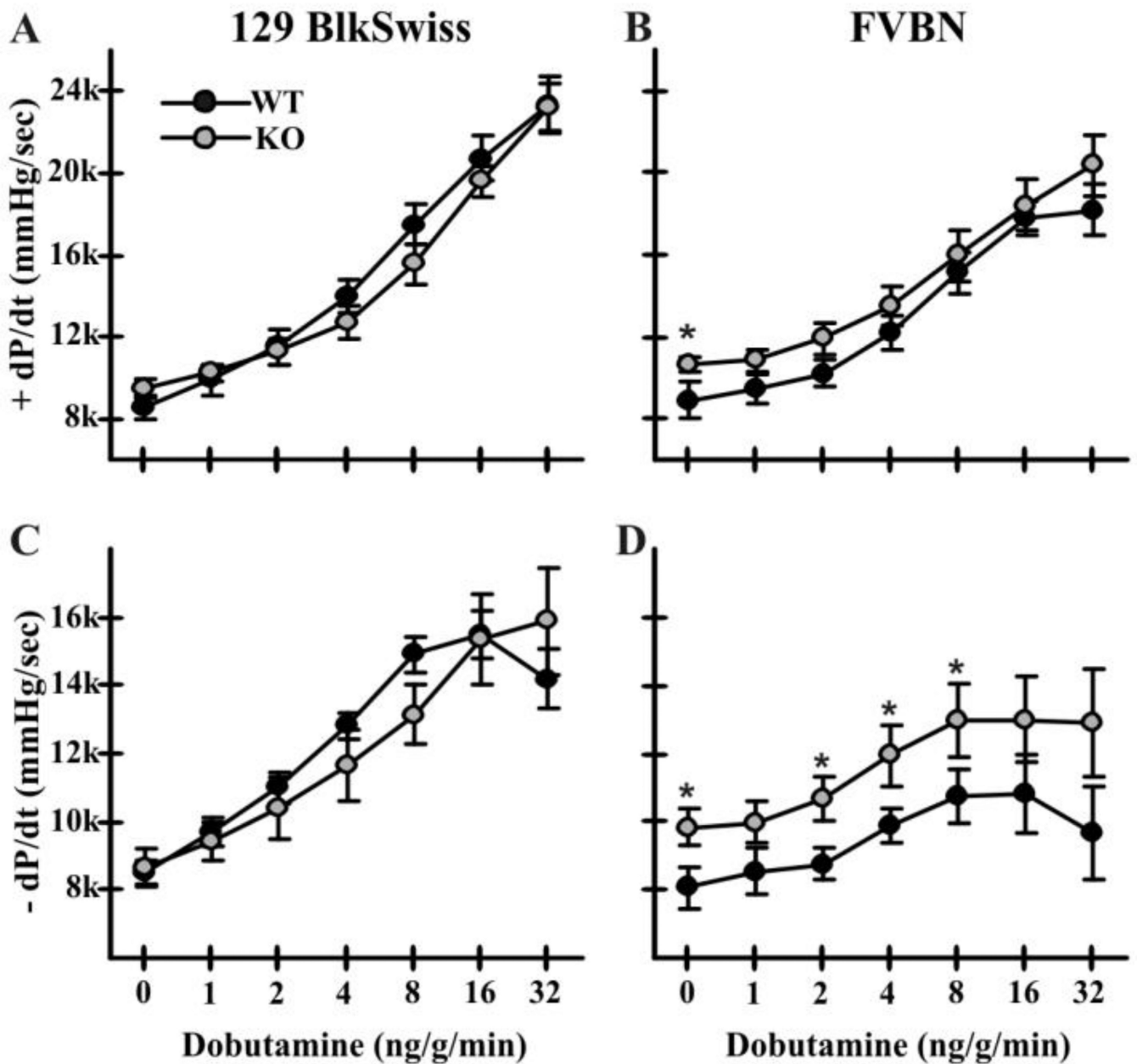


Fig. 1. Cardiovascular performance of WT and *Nhe1*^{-/-} mice. Left ventricular pressure measurements were recorded via a transducer in the left ventricle in WT and *Nhe1*^{-/-} (KO) mice. Data are presented for mice of the 129/Svj and Black Swiss mixed (A,C), and the inbred FVB/N (B,D) genetic backgrounds. Results show dobutamine dose-responses (for β -adrenergic stimulation) in WT and *Nhe1*^{-/-} mice with measurements of maximum dP/dt (+dP/dt; A,B) and minimum dP/dt (-dP/dt; C,D). n = 8 WT and 7 *Nhe1*^{-/-} mice (mixed background); 7 WT and 6 *Nhe1*^{-/-} mice (FVB/N background). Values are means \pm SEM. **P* < 0.05, *Nhe1*^{-/-} vs WT.

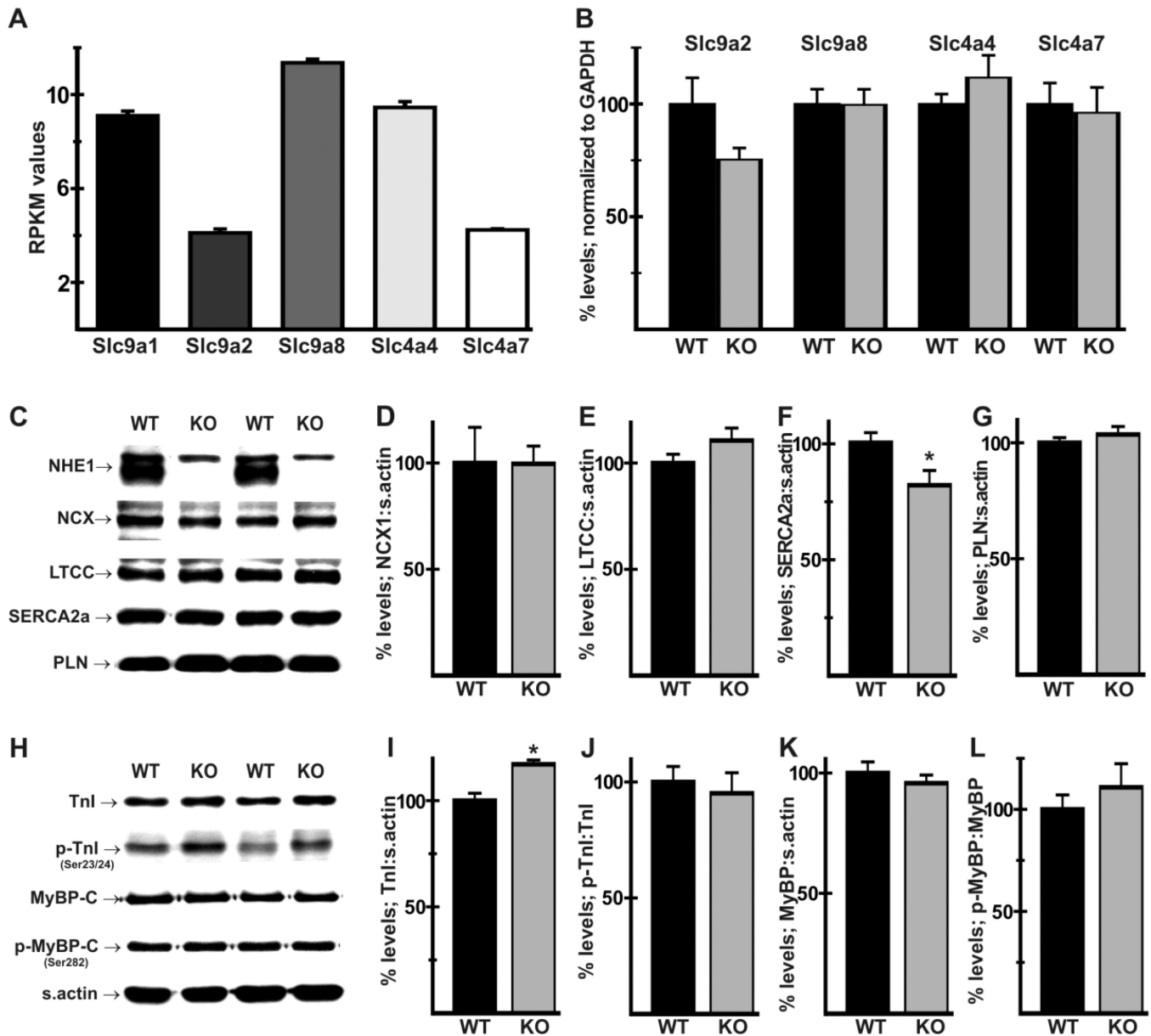
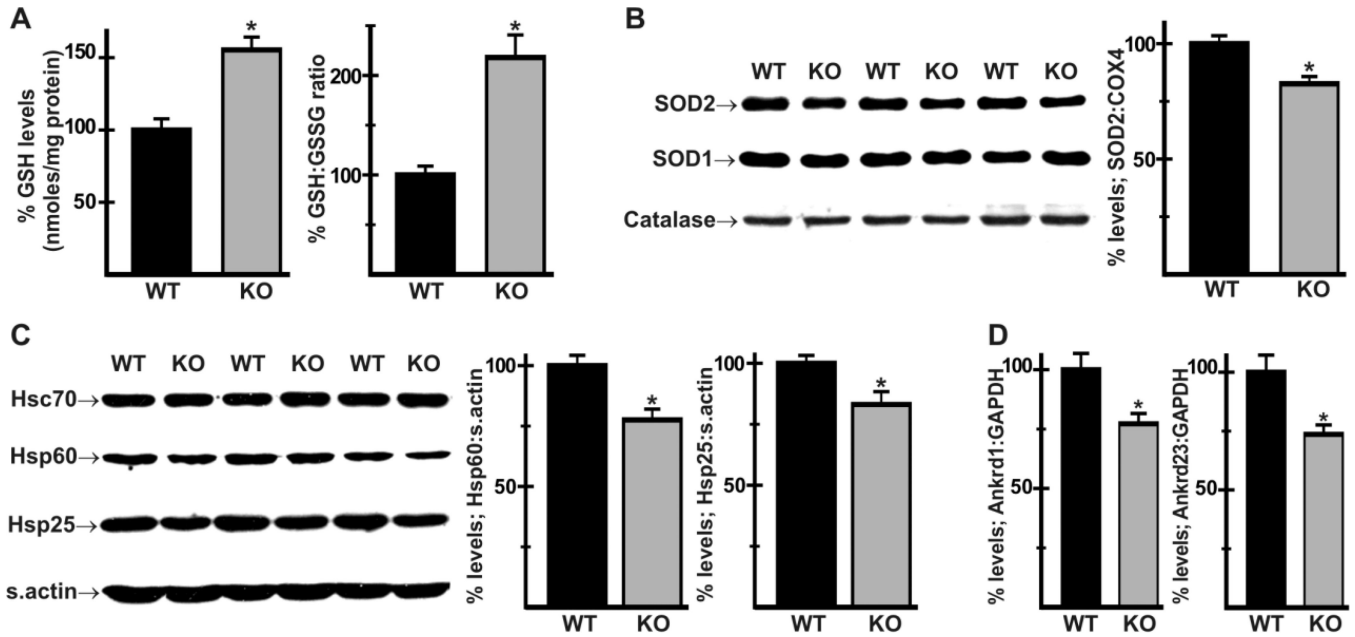


Fig. 2. Effects of NHE1 ablation on expression of Na⁺-dependent transporter mRNAs and Ca²⁺-handling and myofibrillar proteins. RPKM (reads per kilobase of exon per million mapped reads) values (A) for *Slc9a1* (NHE1), *Slc9a2* (NHE2), *Slc9a8* (NHE8), *Slc4a4* (NBCe1), and *Slc4a7* (NBCn1) were computed by RNA-seq analysis of mRNA from FVB/N WT hearts. RT-PCR analysis of total RNA from WT and *Nhe1*^{-/-} (KO) hearts revealed no significant differences in expression of these transporters (B). Immunoblot and densitometric analysis of Ca²⁺ handling (C–G) and myofibrillar (H–L) proteins was conducted using whole heart homogenates to determine levels of NCX1 (D), LTCC α 2 subunit (E), SERCA2a (F), PLN (G), total TnI (I), relative levels of TnI phosphorylated on Ser23/24 (p-TnI, J), total MyBP-C (K), and relative levels of MyBP-C phosphorylated on Ser282 (p-MyBP-C, L). Note the complete ablation of NHE1 in *Nhe1*^{-/-} hearts, but the presence of a non-specific band in both genotypes (C). For each genotype, n=4 for RNA-seq

analysis, 8 for RT-PCR and 4–11 for immunoblot analysis. Values are means \pm SEM. * $P < 0.05$, *Nhe1*^{-/-} vs WT.

**Fig. 3.**

Evidence of reduced oxidative stress, expression of redox related proteins and stress-response genes in *Nhe1*^{-/-} hearts. Analysis of total homogenates of WT and *Nhe1*^{-/-} (KO) hearts using a DTNB/Glutathione reductase-based kit showed increased GSH levels and GSH-GSSG ratios in *Nhe1*^{-/-} hearts (A). Immunoblot and densitometric analyses of mitochondrial and cytosolic fractions (B) showed that SOD2 (normalized to s. actin; normalization to COX4, a mitochondrial enzyme that did not change, gave the same results) was reduced in *Nhe1*^{-/-} hearts, while SOD1 and catalase were unaltered. Immunoblot and densitometric analyses of whole heart homogenates (C) showed reduced levels of heat shock proteins Hsp60 and Hsp25 in *Nhe1*^{-/-} hearts, while Hsc70 expression was unaltered. RT-PCR analysis of total RNA (D) showed that *Ankrd1* and *Ankrd23* mRNAs were down-regulated in *Nhe1*^{-/-} hearts. n=3-11 for each genotype. Values are mean ± SEM. **P* < 0.05, *Nhe1*^{-/-} vs WT.

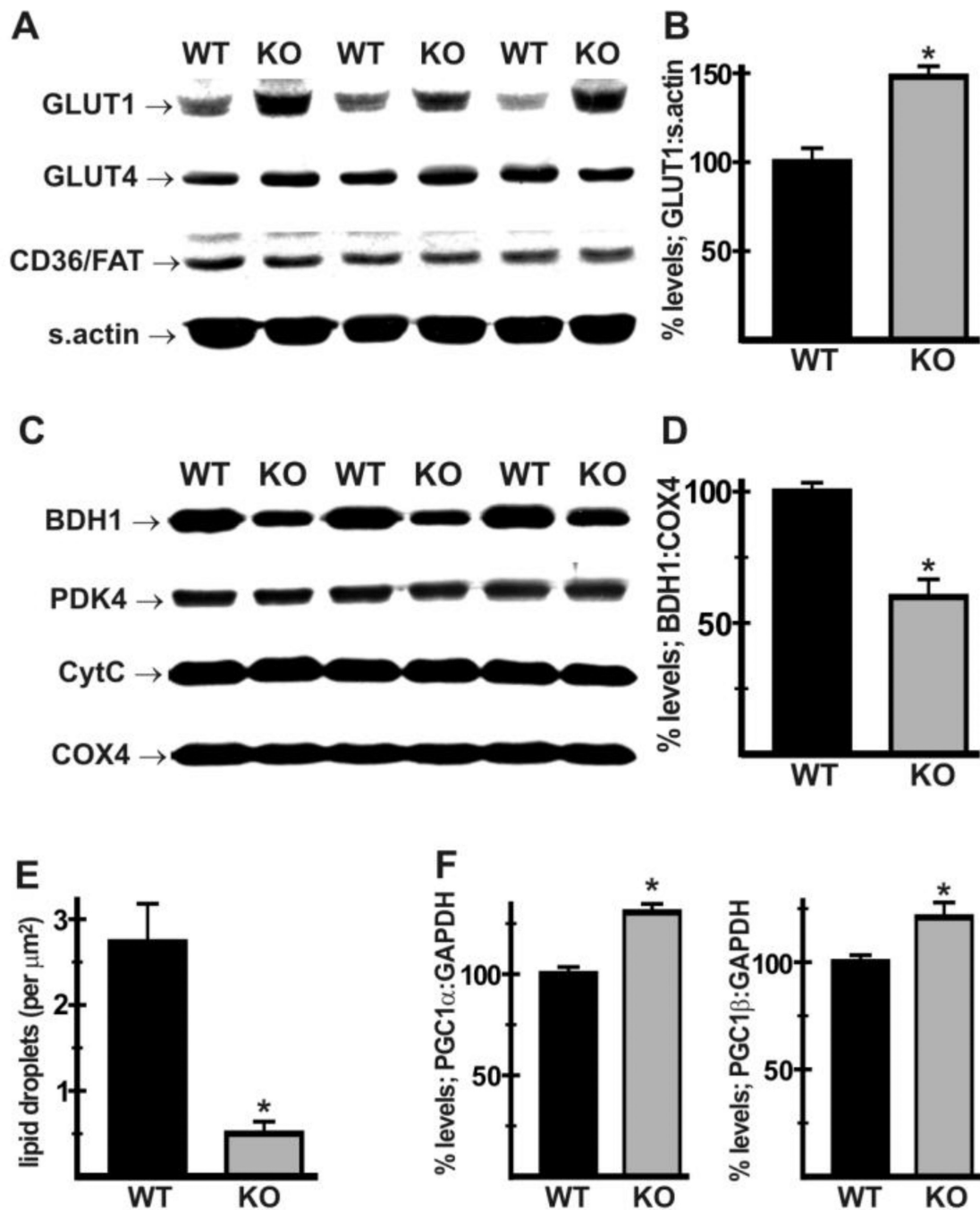


Fig. 4. Effects of NHE1 ablation on regulators of metabolic substrate handling. Immunoblot and densitometric analyses were performed using whole heart homogenates (A,B) and mitochondrial fractions (C,D) from WT and *Nhe1*^{-/-} (KO) hearts. Expression of GLUT1, but not GLUT4 or CD36/FAT, was increased in *Nhe1*^{-/-} hearts (A,B). In mitochondrial fractions, expression of BDH1 (normalized to COX4) was reduced in *Nhe1*^{-/-} hearts, while PDK4, CytC and COX4 were unaltered (C,D). Morphometric analysis of electron micrographs of WT and *Nhe1*^{-/-} hearts showed reduced numbers of lipid droplets in *Nhe1*^{-/-} hearts (E). RT-PCR analysis of total heart RNA samples showed that PGC1 α and

PGC1 β mRNAs were upregulated in *Nhe1*^{-/-} hearts (F). n=4 for each genotype for immunoblots, at least 5 for each genotype for morphometry, and 8 for each genotype for RT-PCR analysis. Values are mean \pm SEM. **P* < 0.05, *Nhe1*^{-/-} vs WT

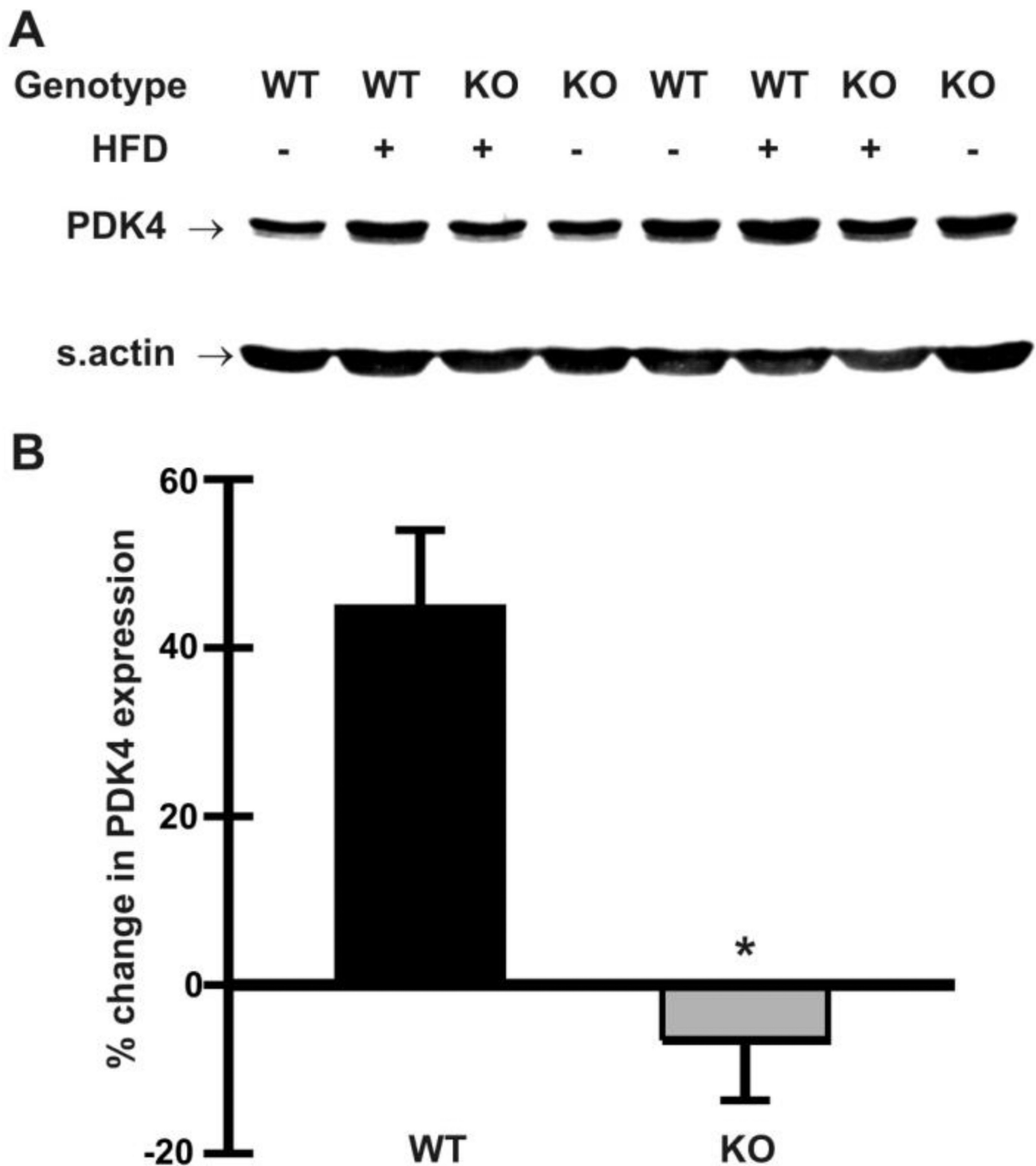


Fig. 5. Effects of high-fat diet on PDK4 expression in *Nhe1*^{-/-} hearts. WT and *Nhe1*^{-/-} (KO) mice were maintained on a normal chow diet or a high-fat diet (HFD, 60 kcal% fat content) for 10 days. Immunoblot (A) and densitometric (B) analyses of whole heart homogenates were carried out to determine changes in expression of PDK4. Cardiac PDK4 expression increased in WT mice but not in *Nhe1*^{-/-} mice, when compared to their chow-fed controls. n=4 for each genotype for each diet type. Values are mean ± SEM. **P* < 0.05, *Nhe1*^{-/-} vs WT.

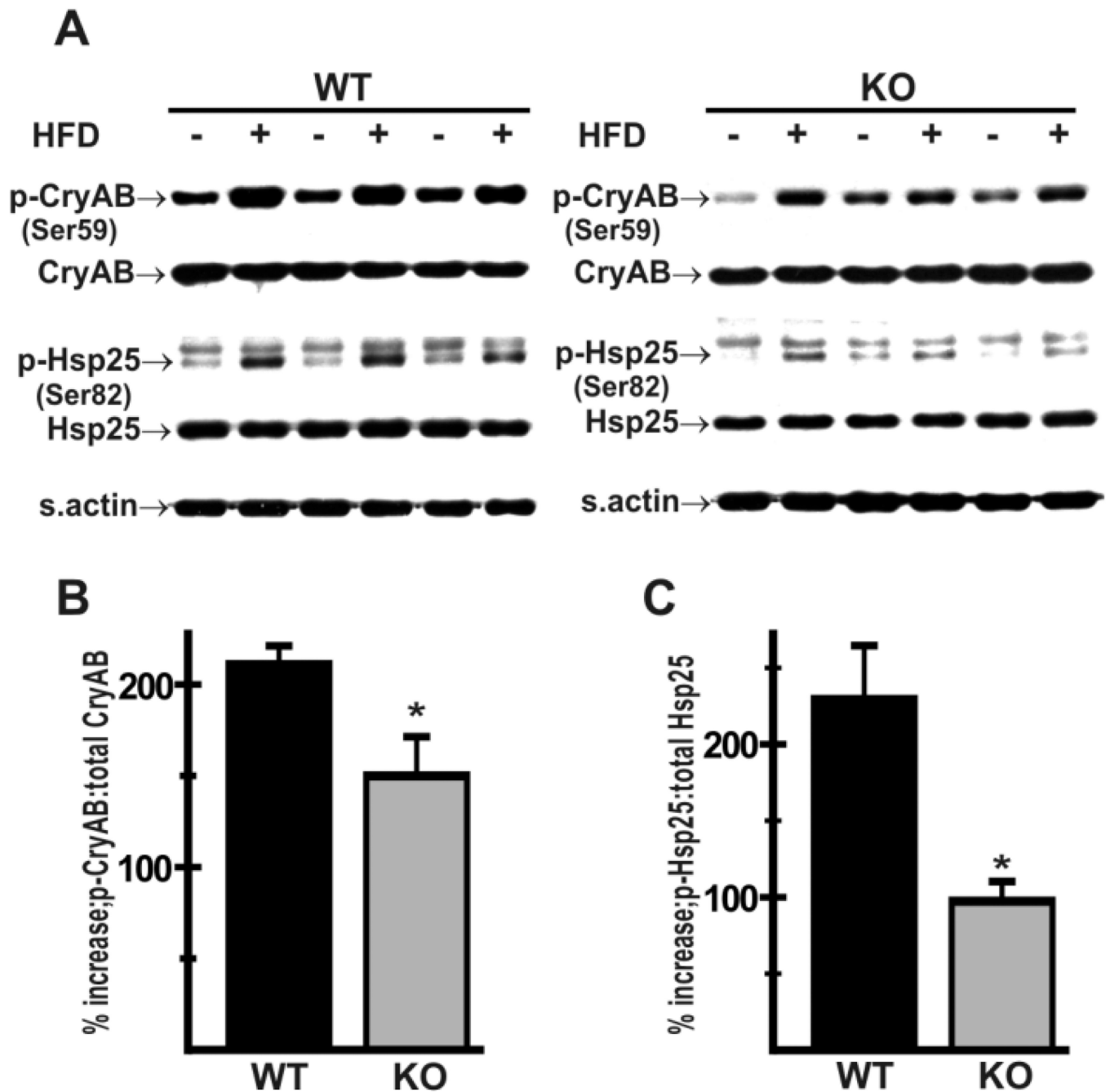
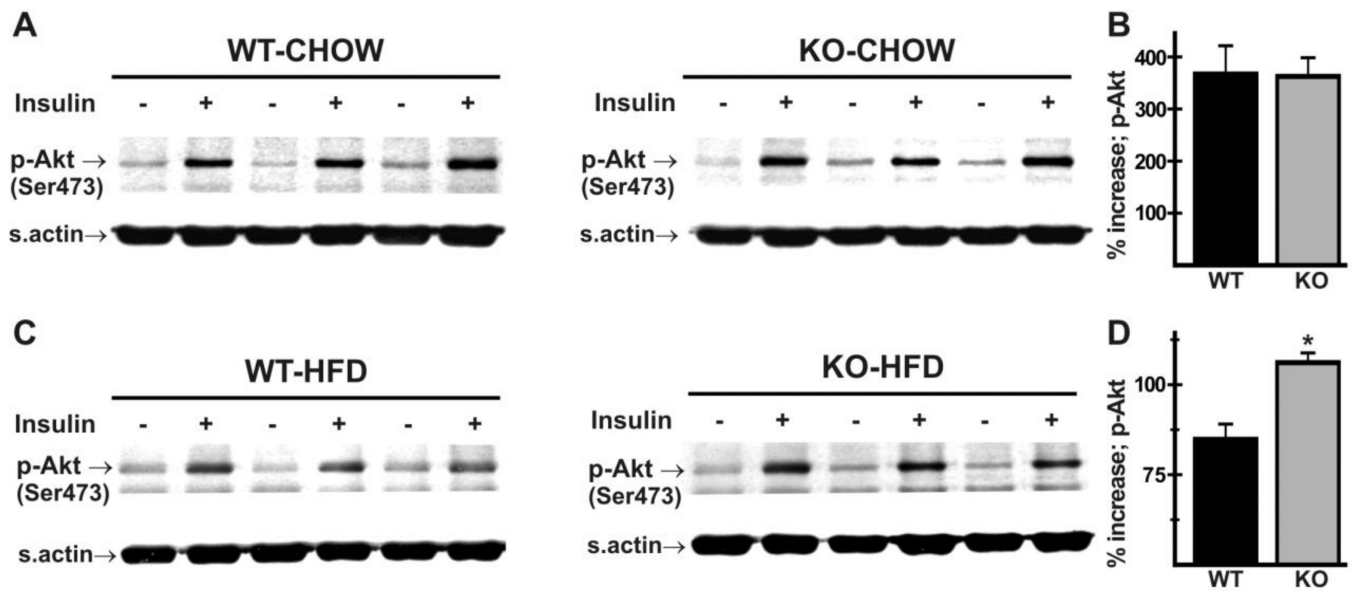


Fig. 6. Effects of high-fat diet on phosphorylation of small stress proteins in *Nhe1*^{-/-} hearts. WT and *Nhe1*^{-/-} (KO) mice were maintained either on a normal chow-diet or a high-fat diet (HFD, 60 kcal% fat content) for 10 days. Immunoblot (A) and densitometric analyses (B,C) of whole heart homogenates were carried out. Compared to levels in chow-fed controls (A), the percent increase in relative phosphorylation of α -Bcrystallin (p-CryAB, Ser59) (B) and Hsp25 (p-Hsp25, Ser82) (C) in response to a high-fat diet was lower in *Nhe1*^{-/-} hearts than in WT hearts. n=4 for each genotype for each diet type. Values are mean \pm SEM. * $P < 0.05$, *Nhe1*^{-/-} vs WT.

**Fig. 7.**

Insulin signaling in WT and *Nhe1*^{-/-} hearts upon chronic exposure to high-fat diet. WT and *Nhe1*^{-/-} (KO) mice were maintained on either normal chow or a high-fat diet (HFD, 60 kcal % fat content) for 8 weeks. Mice were fasted for 2 hours before being administered insulin (13.5 IU/kg bodyweight intraperitoneally). Immunoblot (A,C) and densitometric (B,D) analyses of whole heart homogenates was performed to determine levels of PKB/Akt phosphorylation on Ser473 (p-Akt). In mice on a normal diet, insulin-induced increase in cardiac p-Akt levels was similar in both genotypes (A,B). In HFD mice (C,D), the relative increase in p-Akt levels was greater in *Nhe1*^{-/-} mice. n=3 pairs of each genotype on chow diet, 4 pairs of each genotype on high-fat diet. Values are mean ± SEM. **P* < 0.05, *Nhe1*^{-/-} vs WT.

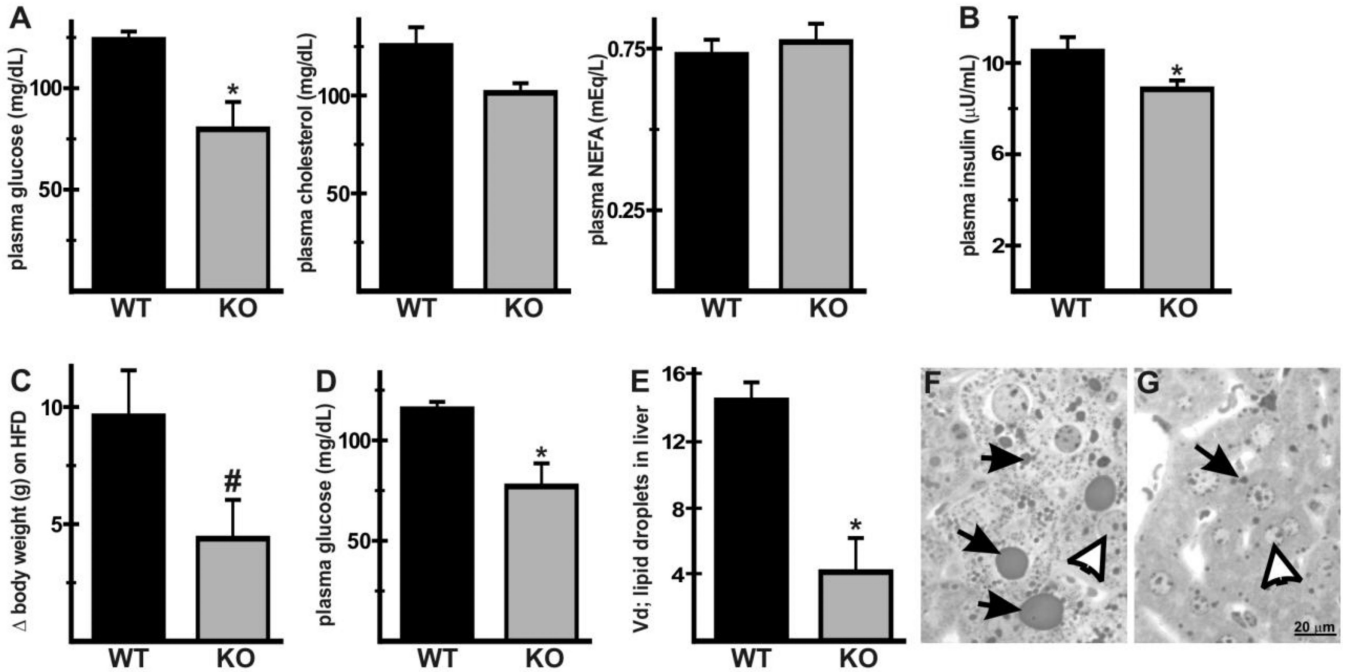


Fig. 8.

Extracardiac effects of NHE1 ablation on metabolic substrate homeostasis. Blood was harvested from WT and *Nhe1*^{-/-} (KO) mice maintained on normal chow after fasting for 2 hours and plasma was analyzed (A,B). Plasma glucose (A) and insulin (B) was lower in *Nhe1*^{-/-} mice, but cholesterol and NEFA levels did not differ significantly between the two genotypes. WT and *Nhe1*^{-/-} mice were fed a high-fat diet (HFD) as described in Fig. 7. HFD-induced gain in bodyweight during the 8-week HFD period (Δ) was lower in *Nhe1*^{-/-} mice (C). Plasma from HFD-fed WT and *Nhe1*^{-/-} mice showed that fasting glucose levels were lower in *Nhe1*^{-/-} mice after 8-weeks of HFD (D). Morphometric analysis of liver samples from HFD WT and *Nhe1*^{-/-} mice showed that the volume density (.Vd) of lipid droplets was lower in *Nhe1*^{-/-} livers than in WT livers (E), and the size of lipid droplets tended to be much larger in WT livers (F) when compared to *Nhe1*^{-/-} livers (G). n=at least 4 for each genotype. Values are mean \pm SEM. * $P < 0.05$, *Nhe1*^{-/-} vs WT; # $P=0.05$, *Nhe1*^{-/-} vs WT.